International Journal of Pharmaceutics 573 (2020) 118834

Contents lists available at ScienceDirect

International Journal of Pharmaceutics

journal homepage: www.elsevier.com/locate/ijpharm

Use of a quartz crystal microbalance platform to study protein adsorption on aluminum hydroxide vaccine adjuvants: Focus on phosphate-hydroxide ligand exchanges

Jean-François Art[a], Patrice Soumillion[b], Christine C. Dupont-Gillain[a,*]

[a] Université catholique de Louvain, Institute of Condensed Matter and Nanosciences, Bio- and Soft Matter Division, Place Louis Pasteur 1/L4.01.10, 1348 Louvain-la-Neuve, Belgium

[b] Université catholique de Louvain, Louvain Institute of Biomolecular Science and Technology, Croix du Sud 4-5/L7.07.06, 1348 Louvain-la-Neuve, Belgium

ARTICLE INFO

Keywords:
Quartz crystal microbalance
Vaccine
Antigen adsorption
Aluminum hydroxide adjuvant
Ligand exchange
Dephosphorylation

ABSTRACT

Aluminum hydroxide (AH) salts are widely used as vaccine adjuvants and controlling antigen-AH interactions is a key challenge in vaccine formulation. In a previous work, we have developed a quartz crystal microbalance (QCM) platform, based on stable AH-coated sensors, to explore the mechanisms of model antigen adsorption. The QCM study of bovine serum albumin (BSA) adsorption at different pH and ionic strength (I) values showed that protein adsorption on AH adjuvant at physiological pH cannot be explained mainly by electrostatic interactions, in contrast with previous reports. Here, we exploit further the developed QCM platform to investigate the role of phosphate-hydroxyl ligand exchanges in the adsorption mechanism of BSA, human serum albumin (HSA) and ovalbumin (OVA) on two commercial AH adjuvants. BSA adsorption decreased on immobilized AH particles previously treated with KH_2PO_4, highlighting the role of exchangeable sites on AH particles in the adsorption process. BSA and OVA were dephosphorylated by treatment with an acid phosphatase to decrease their phosphate content by about 80% and 25%, respectively. Compared to native BSA, adsorption of dephosphorylated BSA decreased significantly on one AH adjuvant at pH 7. Adsorption of dephosphorylated OVA was comparable to the one of native OVA. Further QCM assays showed that phospho-amino acids (PO_4-serine and PO_4-threonine) displaced previously adsorbed BSA and OVA from AH particles in conditions that were depending on the protein and the AH. Taken together, these observations suggest that phosphate-hydroxyl ligand exchange is an important adsorption mechanism of proteins on AH. These results moreover confirm that the developed AH-coated QCM sensors offer a new platform for the study of antigen adsorption, to the benefit of vaccine formulation.

1. Introduction

Vaccine adjuvants are commonly used to trigger a sufficient immune response and a memory effect from vaccines formulated with antigenic subunits of pathogens, such as proteins or polysaccharides, or with pathogen toxoids (Perrie et al., 2008; Mbow et al., 2010; Eppstein et al., 1989). Many types of adjuvants have been studied and used but aluminum-based adjuvants are still the most widespread in human vaccines (Mbow et al., 2010; Eppstein et al., 1989; Sivakumar et al., 2011). Aluminum hydroxide adjuvants were described quite extensively in the literature and are known to present a poorly crystalline AlOOH structure, in which hydroxide groups (OH) are coordinated with aluminum atoms (Hem et al., 1995; Shirodkar et al., 1990). Shirodkar et al. described AH particles as a dynamic system with elemental particles aggregating and disaggregating continuously in suspension, and forming loose aggregates (1–10 μm) considered as the functioning units of adjuvants, *i.e.* the effective structure for antigen adsorption and immune system stimulation (Shirodkar et al., 1990; Morefield et al., 2004). The specific surface area developed by AH adjuvants is found to be around 500 m^2/g (Johnston et al., 2002) and their point of zero charge (PZC) is 11.5 (Rinella et al., 1998). Stability studies showed that AH particles develop more crystalline fractions over time or after autoclave treatment. The higher crystallinity of AH particles leads to a lower AH adjuvant specific surface area and a decreased antigen adsorption capacity (Burrell et al., 1999; Burrell et al., 2000). We recently showed that NaCl, used to adjust the ionic strength (I) of AH suspensions, triggers AH particle aggregation. Indeed, adding 150 mM of NaCl to commercial AH suspensions promoted particle aggregation, thereby

* Corresponding author.
E-mail address: christine.dupont@uclouvain.be (C.C. Dupont-Gillain).

https://doi.org/10.1016/j.ijpharm.2019.118834
Received 22 July 2019; Received in revised form 24 October 2019; Accepted 28 October 2019
Available online 09 November 2019
0378-5173/

decreasing the specific surface area (Art et al., 2017).

Controlling the adsorption of antigenic subunits on aluminum-based adjuvants has been one of the biggest issues of vaccine industry over the past few years (Clausi et al., 2008). Two major adsorption mechanisms of model proteins on AH adjuvants were deduced from adsorption isotherms established through experiments carried out on adjuvant particles in suspension. Electrostatic interactions are thought to be responsible for bovine serum albumin (BSA) adsorption on AH adjuvants at physiological pH (7.4) (Hem et al., 1995; Al-Shakhshir et al., 1995), and ovalbumin (OVA), taken as a model phosphoprotein (phosphate content ranging from 0 to 2 mol PO_4/mol OVA) (Kinoshita-Kikuta et al., 2012), is believed to adsorb to aluminum-based adjuvant particles through ligand exchanges between protein phosphate groups and adjuvant hydroxyl groups (Morefield et al., 2005; Iyer et al., 2003). These adsorption studies suffer however from several drawbacks. First, adsorption is performed in an adjuvant suspension with a complex composition, and the exact role of each component in the adsorption process is difficult to identify. Secondly, the adsorbed amount is determined indirectly by measuring the remaining protein amount in the supernatant after centrifugation. Finally, the range of conditions that were tested (pH, I) were quite narrow, preventing the conclusions to be fully supported by the data.

Recently, we developed a quartz crystal microbalance (QCM)-based method to overcome these drawbacks. We managed to immobilize AH adjuvant particles on QCM sensors without alteration of particle morphology and surface chemistry. The obtained adjuvant layers were also stable over time under water, and stable to changes of ionic strength in their surroundings (Art et al., 2018) and did not show AH particle aggregation in presence of NaCl (Art et al., 2017). Furthermore, the method was sensitive enough to directly monitor BSA adsorption in several conditions of pH and I, thereby overcoming limitations related to indirect evaluation of adsorption.

The QCM platform we developed gave results for BSA adsorption on AH particles, which questioned and partly contradicted earlier results from the literature (Art et al., 2018). Isoresponse maps presenting the adsorption of BSA as a function of pH and the square root of I on two commercial AH adjuvant particles (AH1 and AH2 – see Experimental section) immobilized on QCM sensors are presented in Fig. 1. The highest coverage was observed on AH adjuvant particles at pH 5 in ultrapure water (~ 0 mM), *i.e.* near the IEP of the protein (around 4.8) (Salis et al., 2011), as expected (Norde, 2008). Adsorption of BSA in condition of screened electrostatic repulsion is observed on AH particles, at pH 3 and high I, and can be explained by surface-induced and pH-induced protein conformation changes (Nakamura et al., 1997; Jachimska and Pajor, 2012) and by the heterogeneous charge distribution at the protein surface (Jachimska et al., 2016; Nattich-Rak et al., 2017). It was moreover shown that adsorption by ligand exchange can overcome repulsive electrostatic forces (Morefield et al., 2005; Jiang et al., 2006), which could be another explanation for BSA adsorption at pH 3. Furthermore, the protonation of OH groups at the surface of AH particles at pH 3 (leading to OH_2^+ groups) could also facilitate ligand exchanges with PO_4 groups of BSA through the release of a water molecule since OH_2^+ groups are easier to exchange than OH groups.

The results obtained at pH 7 caught our attention. At this pH, BSA and AH particles are respectively negatively and positively charged. In ultrapure water (I ~ 0 mM), BSA poorly adsorbs on both AH adjuvants, even though attractive electrostatic interactions must be at play. The microenvironment pH, which may be up to two units higher than the bulk pH (Wittayanukulluk et al., 2004), may explain this low adsorption. When a low salt concentration is added, BSA adsorption is higher, and does not vary further with increasing I, excluding a major contribution of coulombic interactions in BSA adsorption. These data, obtained by direct QCM measurements on immobilized AH particles, are in contradiction with previously published conclusions regarding BSA adsorption on AH particles, which attributed adsorption mainly to electrostatic interactions (Al-Shakhshir et al., 1995). The BSA adsorption decrease observed by Al-Shakhshir et al. at pH 7.4 while increasing I from 60 to 750 mM in NaCl was moreover not observed here. These previous data were however obtained from indirect measurements in suspension (Al-Shakhshir et al., 1995), at I values (60 mM, 250 mM and 750 mM) leading to very short and similar Debye lengths that did not allow electrostatic interactions to be properly challenged.

The mechanism of BSA adsorption on AH particles is thus still not completely understood, but may be related to ligand exchanges (Morefield et al., 2005; Iyer et al., 2003). Indeed, BSA (P02769 (ALBU_BOVIN) – Uniprot Consortium) is a globular protein of 69 kDa, in which the phosphate content may range from 0 to 10 mol PO_4/mol BSA. The phosphorylated residues (phosphoserine and/or phosphothreonine) could play a role in BSA adsorption through ligand exchanges. The question of the influence of phosphate-hydroxyl ligand exchanges is not only relevant for BSA adsorption, but more generally applies to protein or other phosphate-containing antigen adsorption on AH adjuvants.

This work aims at using the QCM platform developed previously, based on stable and reproducible surfaces coated with immobilized AH particles, to explore the involvement of PO_4-OH ligand exchanges in the adsorption of three proteins (BSA, HSA, OVA) taken as model antigens. These proteins feature different phosphoserine and phosphothreonine contents. The influence of phosphorylated residues in a protein on its adsorption mechanisms on AH adjuvant particles was studied in various conditions of pH and I. Native proteins were adsorbed on immobilized AH particles treated with KH_2PO_4 to decrease the number of surface OH groups available for ligand exchanges. Solutions of free phosphorylated serine and threonine were brought in contact with BSA and OVA molecules previously adsorbed on immobilized AH adjuvant particles, to

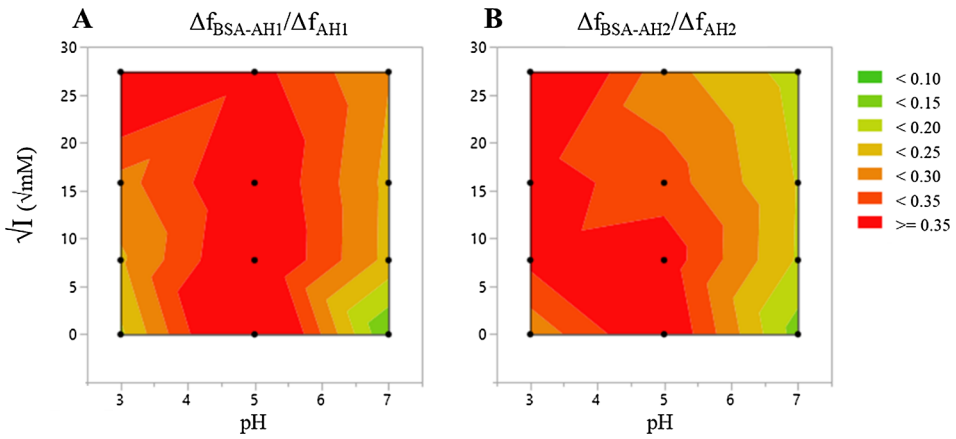

Fig. 1. BSA adsorption measured by QCM on immobilized AH1 (A) and AH2 (B) adjuvant particles and presented as a function of pH and square root of ionic strength. Black dots are means of experimental data (n = 5), between which color lines are drawn using a triangulation method and linear interpolation. Reprinted with permission from (Art et al., 2018), copyright 2018 American Chemical Society. (For interpretation of the references to colour in this figure legend, the reader is referred to the web version of this article.)

potentially trigger protein desorption through ligand exchanges between adjuvant particles and free phospho-amino acids. BSA and OVA molecules were also dephosphorylated using an acid phosphatase, and further adsorbed on immobilized AH particles at different pH and I. Adsorption of native and dephosphorylated protein molecules were compared to highlight the importance of phosphate groups in the adsorption mechanisms of these proteins. Taken together, the generated results increase the knowledge on adsorption mechanisms involved in protein adsorption on AH adjuvant particles during vaccine formulation.

2. Experimental section

2.1. Materials

Two commercial aluminum hydroxide adjuvants were used. ALHYDROGEL® "85" 2% - Ph. Eur. (AH1) was kindly provided by BRENNTAG (Brenntag Biosector, Denmark), and REHYDRAGEL® LV (AH2) was purchased from General Chemical (NJ, USA). Both adjuvants consist of a suspension of particles in water. These adjuvants were characterized in previous works (Art et al., 2017; Art, 2018). They showed very similar crystallinity, surface chemical composition, particle size and morphology, relative phosphophilicity and surface specific area. AH2 was however found to form a gel more readily than AH1 upon salt addition.

Bovine serum albumin (BSA ≥ 96%), human serum albumin (HSA ≥ 96%), and albumin from chicken egg white (ovalbumin (OVA) ≥ 98%) were selected (Sigma Aldrich, St. Louis, MO, USA) as model protein antigens and were dissolved at 200 μg/mL in ultrapure water. Two phospho-amino acids (O-phospho-L-threonine (PO_4-Thr) and O-phospho-L-serine (PO_4-Ser)) and the corresponding native amino acids (L-threonine (Thr) and L-serine (Ser)) were purchased from Sigma Aldrich (St. Louis, MO, USA). The amino acids (AA), on the one hand, and phospho-amino acids (PO_4-AA), on the other hand, were dissolved together in ultrapure water at 23 μg/mL of (PO_4-)Thr and 32 μg/mL of (PO_4-)Ser (55 μg/mL in total of AA or PO_4-AA). BSA can theoretically have up to 10 PO_4 residues (6 PO_4-Ser and 4 PO_4-Thr). Based on these mass concentrations, the molar concentration of free PO_4-AA in a 55 μg/mL solution is ten times higher than the maximum one of PO_4-residues of BSA in a 200 μg/mL solution, and the molar concentration of free AA molecules (serine and threonine) is around 17 times higher than the maximum one of PO_4-residues of BSA in a 200 μg/mL solution. Ten times more concentrated solutions (550 μg/mL in PO_4-AA or AA) were also prepared. Potato acid phosphatase (PAP) (lyophilized powder, ≥ 0.5 unit/mg solid) was purchased from Sigma Aldrich (St. Louis, MO, USA). PAP was dissolved at 20 μg/mL in ultrapure water. KH_2PO_4 was purchased from Sigma Aldrich (St. Louis, MO, USA) and dissolved at 0.2 M in ultrapure water. When needed, the ionic strength I was adjusted with NaCl (Sigma Aldrich, St. Louis, MO, USA) and pH was adjusted with HCl or NaOH and measured with pH-indicator strips (pH 1–14 and pH 2–9, Merck, Darmstadt, Germany).

2.2. AH particles immobilized on QCM sensors

AH particles were immobilized on quartz crystal microbalance sensors (4.95 MHz AT-cut gold-coated quartz sensors, Q-Sense, Stockholm, Sweden). QCM sensors were washed with a 2:1 (v:v) mixture of H_2SO_4 95% and H_2O_2 30% w/w (VWR International, Leuven, Belgium), rinsed with ultrapure water, and exposed during 15 min to UV/O_3 (UVO cleaner, Jelight Company, USA) before coating. Gold surfaces were coated by spin-coating of 150 μL of pH-adjusted AH suspension (pH 4 for AH1 suspension and pH 6 for AH2 suspension) with a WS-400B-6NPP/Lite spin-coater (Laurell Technologies Corporation, North Wales, USA) during 30 s at 10,000 rpm. Each AH-covered sensor was then submitted two times to, successively, 15 min under a 50 μL/min flow of NaCl 750 mM solution and 15 min under a 50 μL/min flow of ultrapure water in the QCM device. These rinsing steps are needed to ensure the stability of the coating as previously shown (Art et al., 2018).

2.3. BSA adsorption monitored on KH_2PO_4-treated AH particles

QCM sensors were covered with AH particles as described here above. After the NaCl treatment, AH-covered sensors were submitted to 30 min of 50 μL/min of KH_2PO_4 at 0.2 M. BSA was then adsorbed on KH_2PO_4-treated AH particles at pH 3, 5 and 7 and I of ~0 mM (ultrapure water), 60, 250 and 750 mM in NaCl, as previously described in details (Art et al., 2018).

2.4. QCM experiments of model protein desorption by phosphorylated amino acids

Protein adsorption experiments were conducted for 1 h at pH 3, 5 and 7 and I of ~0 mM (ultrapure water), 60, 250 and 750 mM in NaCl, as previously described in details (Art et al., 2018), and the AH-coated sensors with adsorbed proteins were then flowed with solutions of free PO_4-AA or AA to monitor desorption, as detailed in Supporting Information (SI-1) and schematized in Fig. S-1 (SI).

The "Q-stomize" software, developed in the laboratory by Mc Evoy (2012), enabled to accurately extract frequency shifts (Δf) and dissipation shifts (ΔD) over selected time periods, with respect to the baseline recorded in water. The average of the normalized 3rd, 5th and 7th overtones was used to compute the protein adsorption frequency shifts ($\Delta f_{prot\text{-}AH}$ in Fig. S-1). Adsorption results were expressed under the form of Δf values and were normalized by the frequency shift representing the immobilized AH amount (Δf_{AH} as defined in Art et al., 2018). This enables the comparison of results from different experiments, *i.e.* obtained on different sensors. An isoresponse map of $\Delta f_{prot\text{-}AH}/\Delta f_{AH}$ ratios presented as a function of pH and the square root of I was finally drawn with the JMP software (JMP 12.0, SAS Institute, NC, USA). This contour plot was generated by a triangulation method and linear interpolation of experimental data. Note that in such map, each black dot corresponds to the mean of experimental data acquired in the given pH and I condition, and the number of repetitions is given in the Figure caption (n = 3 in most cases). For the sake of readability of the isoresponse maps, the standard deviations are reported in Tables found in the Supporting Information section.

The desorption due to AA or PO_4-AA (Δf_{deso}) was measured as the difference between the frequency shift attributed to protein adsorption ($\Delta f_{prot\text{-}AH}$) and the frequency shift attributed to the remaining protein amount after desorption ($\Delta f_{prot.\ rem.}$ in Fig. S-1). Isoresponse maps of $\Delta f_{deso}/\Delta f_{prot\text{-}AH}$ ratios, which represent the relative desorption of model proteins by free (PO_4-)AA, are also presented as a function of pH and the square root of I, using the JMP software.

2.5. Adsorption of dephosphorylated model proteins

BSA and OVA were dephosphorylated by mixing 5 mL of the protein solution at 200 μg/mL with 0.5 mL of potato acid phosphatase (PAP) at 20 μg/mL (PAP final concentration is equal to 1% of BSA or OVA concentration). The obtained solution was adjusted at pH 7 with NaOH, to work in conditions described in the literature (Bingham et al., 1976), and agitated on an orbital shaker (PSU-10i, BIOSAN, Riga, Latvia) at 220 rpm during 1 h. After the 1 h dephosphorylation step, pH and I of the protein solutions were fixed at the chosen conditions for adsorption experiments (pH 3, 5 or 7 and I of ~0, 60, 250, 750 mM) with respectively HCl or NaOH, and NaCl. The treated protein solutions (dephosphorylated BSA – dBSA, or dephosphorylated OVA – dOVA), still containing PAP at 1% of their initial concentration, were used for adsorption on immobilized AH particles in QCM directly after pH and I adjustment. The adsorption of PAP alone at 2 μg/mL, *i.e.* close to the concentration used for treatment, at the chosen pH and I was monitored

by QCM as a control.

2.6. Evaluation of protein phosphate content and of protein dephosphorylation by inductively coupled plasma-atomic emission spectroscopy (ICP-AES)

10 mL of BSA or OVA at 10 mg/mL were dephosphorylated by treatment with 1 mL of PAP at 1 mg/mL, during 1 h at pH 7. After the dephosphorylation step, both BSA + PAP and OVA + PAP solutions were centrifuged using Vivaspin 2 centrifugal concentrators (Sigma Aldrich, St. Louis, MO, USA) with a molecular mass cut-off (MWCO) of 5,000 Da. Centrifugation was conducted at 7000*g* (~7750 rpm on Heraeus Multifuge X1R, Thermo Scientific, Osterode, Germany). The amount of cleaved phosphate groups was measured in the filtrate, while phosphate groups remaining in model proteins were measured by recovery of the proteins from the filter in 10 mL ultrapure water. The phosphorus content was measured by ICP-AES on a Thermo Scientific iCap 6500 device (Waltham, Massachusetts, USA) powered with argon. This content was compared to the initial phosphorus content in 10 mL of BSA or OVA solutions at 10 mg/mL, and in 10 mL of PAP solution at 0.1 mg/mL. Note that, here, more concentrated solutions of BSA or OVA and PAP were used to be above the limit of detection of ICP-AES. The BSA or OVA to PAP ratio was however kept identical to the one used to produce dBSA and dOVA solutions for adsorption studies.

3. Results and discussion

3.1. Model protein adsorption on immobilized AH particles

BSA, HSA and OVA were adsorbed at pH 3, 5 and 7 and I of ~0 mM (ultrapure water), 60 mM, 250 mM, and 750 mM in NaCl on immobilized AH particles. BSA adsorption was already presented and discussed in the Introduction section (see Fig. 1 and related text). To sum up, the highest coverage was observed on AH adjuvant particles at pH 5 in ultrapure water (~0 mM), *i.e.* near the IEP of the protein (Salis et al., 2011). Adsorption of BSA in conditions of screened electrostatic repulsion was observed at pH 3 and high I. At pH 7, where BSA and AH particles are oppositely charged, BSA adsorption was shown not to be driven by electrostatic interactions, as it was not decreased by increasing ionic strength. HSA adsorption on both AH adjuvants was also studied and the results are presented in SI-2 (Fig. S-2, Tables S-1 and S-2). HSA, which has the same number of amino acid residues that could be phosphorylated (10 mol PO_4/mol HSA, P02768 (ALBU_HUMAN) – Uniprot Consortium) and has a similar sequence (76% of sequence identity), mass, size and shape compared to BSA, behaves very similarly as BSA on both AH adjuvants.

The adsorption of OVA is different from the one of the two other albumins. OVA is a smaller protein (43 kDa) and has a maximum of only two phospho-amino acid residues in its sequence. OVA adsorption on both AH adjuvants immobilized on QCM sensors is presented in Fig. 2 (note that each black dot represents a mean over 3 repetitions), while $\Delta f_{OVA\text{-}AH}/\Delta f_{AH}$ values and standard deviations are reported in SI-3 (Tables S-3 and S-4). The results clearly show that (i) OVA has a behavior that markedly differs from the one of BSA and HSA, and (ii) OVA adsorption depends on the adjuvant used (AH1 vs AH2), in contrast with the very similar behavior of both adjuvants towards BSA and HSA.

On AH1 particles, OVA adsorbs in high amount at pH 5 in presence of NaCl. Adsorption at pH 5 is comparatively lower in ultrapure water. Adsorption at pH 3 and 7 is very low in ultrapure water and strongly increases with increasing I. Adsorption results obtained at pH 7 cannot be explained by electrostatic interactions, as OVA adsorbed amount increases with I. Whatever the pH and I values, ligand exchanges could also drive OVA adsorption on AH1 particles, as previously suggested (Morefield et al., 2005). Furthermore, OVA adsorption at pH 3 and 7 is much higher than BSA or HSA adsorption on the same adjuvant particles (see Fig. 1 and Fig. S-2 in SI) despite the lower size of the protein, pointing to a higher affinity of OVA for AH1 particles.

On AH2 adjuvant, ovalbumin adsorbs quite well at pH 5, but less than on AH1 adjuvant and also less than BSA and HSA at pH 5 on AH2 particles. The same behavior as BSA and HSA is observed at pH 3, *i.e.* adsorption increases with I. At pH 7, OVA adsorption is low in ultrapure water, then increases in presence of NaCl to a constant value, which is however markedly lower than on AH1 adjuvant. The affinity of OVA for AH2 adjuvant is then lower than for AH1. If OVA adsorbs to AH particles mainly through ligand exchanges, this result suggests that AH2 adjuvant particles are less likely to exchange OH groups by PO_4 groups of proteins than AH1 particles at pH 7.

OVA adsorption on AH1 particles at pH 5 and 7 importantly differs from adsorption results obtained on AH2 adjuvant in the same conditions. This result was not observed for BSA/HSA adsorption (Fig. 1/Fig. S-2), which could be explained by the involvement of different adsorption mechanisms according to the protein.

3.2. Phosphate content of model proteins and dephosphorylation by PAP

Based on their sequence, the maximum phosphate content in BSA is 10 mol PO_4/mol BSA, under the form of 6 PO_4-serine residues and 4 PO_4-threonine residues distributed as shown in Fig. S-3 A and B (SI), and 2 mol PO_4/mol protein in OVA, with 2 PO_4-serine residues as represented in Fig. S-3C and D (SI).

The phosphorus concentration (in ppm) of 10 mg/mL BSA or OVA solutions was measured by ICP-AES and can be found in the first line of Table 1, and it is expressed in mol PO_4/mol protein in the second line of Table 1. The BSA solution contains 0.06 mol of PO_4 per mole of BSA. It means that 0.6% of all the serine and threonine residues that could be modified are effectively phosphorylated. In other words, at least 94% of

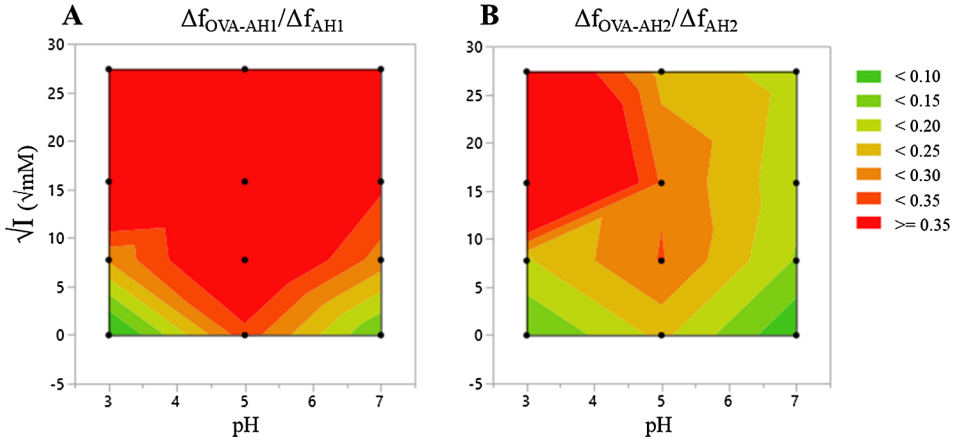

Fig. 2. OVA adsorption measured by QCM on immobilized AH1 (A) and AH2 (B) particles and presented as a function of pH and square root of ionic strength. Black dots are means of experimental data (n = 3), between which color lines are drawn using a triangulation method and linear interpolation. (For interpretation of the references to colour in this figure legend, the reader is referred to the web version of this article.)

Table 1
Phosphorus (P) amount in ppm measured by ICP-AES in 10 mg/mL BSA and OVA solutions, and computed in mol PO_4/mol protein. Evaluation of the dephosphorylation of BSA and OVA by treatment with PAP at pH 7 (in %), both by measuring the released PO_4 and the PO_4 remaining in the proteins. Standard deviations are presented in italic (n = 3). Note that PAP solution at 0.1 mg/mL (control solution) contains 0.04 *(0.02)* ppm of P.

	BSA	OVA
P in native protein [ppm]	0.29 *(0.12)*	5.91 *(0.82)*
P in native protein [mol PO_4/mol protein]	0.06 *(0.03)*	0.82 *(0.11)*
PO_4 released by PAP [%]	80 *(30)*	24 *(3)*
PO_4 remaining in dephosphorylated proteins [%]	34 *(8)*	61 *(6)*

BSA molecules are not phosphorylated at all. Several phosphate distributions are possible, from a more likely situation in which 6 BSA molecules bearing one phosphate group each are surrounded by 94 PO_4-free BSA molecules, to a less likely situation in which one BSA molecule is entirely phosphorylated, with 10 PO_4-residues, and is surrounded by ~166 PO_4-free BSA molecules.

The phosphate content of OVA is much higher, around 0.8 mol of PO_4 per mole of OVA. In this case, 40% of the serine and threonine residues are effectively modified (max 2 mol PO_4/mol OVA) (Kinoshita-Kikuta et al., 2012). Again, this may result in a variety of phosphate group distributions, with two extreme cases as follows. Either 80 OVA molecules out of a hundred contain one phosphorylated residue each, or less likely, 40 OVA molecules are completely phosphorylated (max 2 PO_4-residues/OVA), and the 60 others are PO_4-free. In a previous study, the phosphorylation level of OVA was found to be about twice higher, with about two third and one third of molecules containing two or one PO_4-residues, respectively, and only a very few PO_4-free molecules (Kinoshita-Kikuta et al., 2012). In all cases, only the Ser 68 residue, present at the surface of the protein, is expected to be able to immediately perform ligand exchange with AH particles upon adsorption or to be dephosphorylated upon the action of PAP. Since Ser 344 is located inside the protein structure (Fig. S-3C and D in SI), it would indeed need OVA conformation changes to perform adsorption through ligand exchanges (Shi et al., 2001) or to be reached by the enzyme.

Results of BSA and OVA dephosphorylation by PAP are presented in Table 1. Note that the phosphorus content was measured in a 0.1 mg/mL PAP solution as a control. PAP theoretically does not contain any phosphorylated residues in its sequence, and the obtained phosphorus content, coming from contamination or experimental error, is thus very low (0.04 ppm).

The treatment of BSA and OVA solutions by PAP releases around 80% of the PO_4 groups from BSA molecules, and 24% of PO_4 from OVA molecules (third line in Table 1), which confirms that treating BSA and OVA solutions with PAP effectively decreases the content of PO_4-residues in the proteins, and allows dBSA and dOVA solutions to be obtained. This should allow the role of ligand exchanges on the adsorption of these proteins to be clarified. To further check the dephosphorylation procedure, the phosphate content was also measured on the recovered dephosphorylated protein molecules (after separation from the liquid phase), as shown in the fourth line of Table 1. The sum of the PO_4 fraction found in the recovered protein molecules and the one constituted by released PO_4 groups is expected to be close to 100%, as observed. Somewhat lower values may be due to the impossibility to recover all protein molecules from the filter (Mc Evoy, 2012). This sum is slightly above 100% for BSA, which can be explained by the very low PO_4 amounts measured in this protein, leading to a higher sample-to-sample variability.

3.3. Adsorption of dephosphorylated model proteins (dBSA and dOVA)

dBSA and dOVA (~200 µg/mL) were adsorbed at pH 3, 5 and 7 and I of ~0, 60, 250 and 750 mM in NaCl on AH particles immobilized on QCM sensors. As explained in the experimental section, dBSA or dOVA were adsorbed together with both PAP (used for dephosphorylation) and the released PO_4 groups. PAP has a size and molecular mass close to the one of dBSA and dOVA, thus making their separation difficult. To avoid dealing with their separation, PAP at a concentration of 1.8 µg/mL (corresponding to 1% of the BSA or OVA concentration used for adsorption experiments) was used to treat BSA or OVA, and control experiments were carried out to check that PAP at such a low concentration does not interfere with dBSA or dOVA adsorption on AH particles (SI-5 and Fig. S-4).

The amount of PO_4 released from the BSA molecules by treatment with PAP was shown to be around 80% of the initial amount. If phosphate ligand exchange is the principal driving force for BSA adsorption, this dephosphorylation level is in principle high enough to affect BSA adsorption, especially if BSA molecules bearing a single PO_4 group became PO_4-free. Fig. 3 presents isoresponse maps of the ratio between dBSA adsorption (expressed as $\Delta f_{dBSA\text{-}AH}/\Delta f_{AH}$) and BSA adsorption (expressed as $\Delta f_{BSA\text{-}AH}/\Delta f_{AH}$ and presented in Fig. 1) in given conditions of pH and I on both AH adjuvants. In these maps, grey (or slightly colored) areas correspond to the absence of effect of protein dephosphorylation, while blue and red areas respectively correspond to a decrease or an increase of adsorption attributed to dephosphorylation. Mean values (isoresponse maps and $\Delta f_{dBSA\text{-}AH}/\Delta f_{AH}$ ratios) and the corresponding standard deviations for the adsorption of dBSA on both AH adjuvants are shown in SI-6 (Fig. S-5, Tables S-5 and S-6), while the mean values and standard deviations for BSA adsorption were presented previously (Fig. 1) (Art et al., 2018). dBSA adsorption on AH1 is similar to BSA adsorption in each condition of pH and I, as shown in Fig. 3 A, meaning that the dephosphorylation process does not significantly alter BSA adsorption. This result suggests that ligand

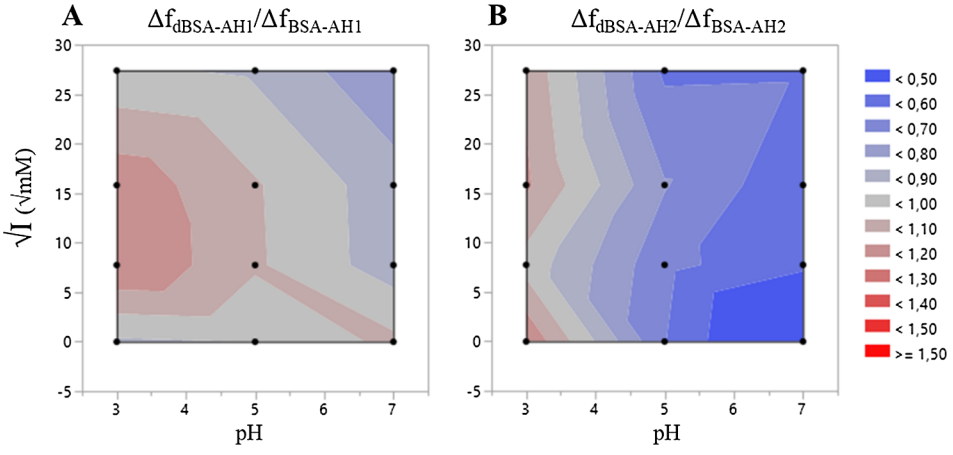

Fig. 3. Ratio of dBSA and BSA adsorption frequency shifts on (A) AH1 and (B) AH2 adjuvant measured on AH-coated QCM sensors and presented as a function of pH and square root of ionic strength. Black dots are means of experimental data (n ≥ 3), between which color lines are drawn using a triangulation method and linear interpolation. (For interpretation of the references to colour in this figure legend, the reader is referred to the web version of this article.)

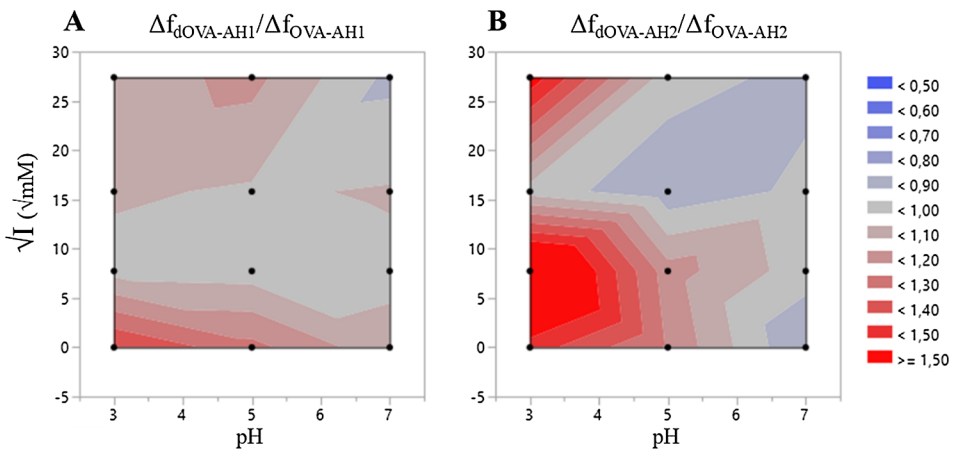

Fig. 4. Ratio of dOVA and OVA adsorption frequency shifts on (A) AH1 and (B) AH2 adjuvant measured on AH-coated QCM sensors and presented as a function of pH and square root of ionic strength. Black dots are means of experimental data (n ≥ 2), between which color lines are drawn using a triangulation method and linear interpolation. (For interpretation of the references to colour in this figure legend, the reader is referred to the web version of this article.)

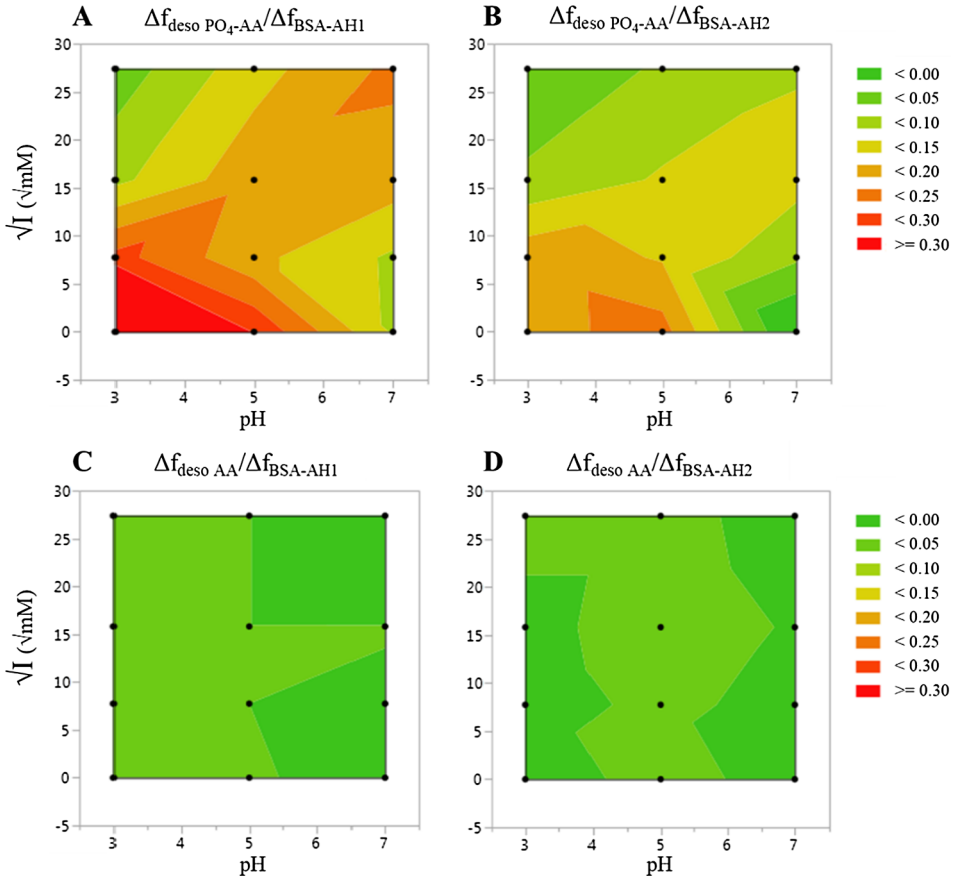

Fig. 5. A-B: BSA desorption measured as the ratio of BSA desorbed after treatment with the 550 µg/mL PO_4-AA solution ($\Delta f_{deso\ PO4\text{-}AA}$) and BSA adsorption frequency shift (Δf_{BSA}) on (A) AH1 and (B) AH2 particles. Black dots are means of experimental data (n = 2). **C-D**: BSA desorption measured after treatment with a 550 µg/mL AA solution ($\Delta f_{deso\ AA}$) and related to BSA adsorption (Δf_{BSA}) on (C) AH1 and (D) AH2 particles. Black dots present experimental data (n = 1). Ratios are presented as a function of pH and square root of ionic strength. Color lines are drawn between experimental data using a triangulation method and linear interpolation of experimental data. (For interpretation of the references to colour in this figure legend, the reader is referred to the web version of this article.)

exchange solely cannot explain BSA adsorption behavior.

On immobilized AH2 particles, dBSA adsorption is not significantly altered at pH 3 compared to BSA adsorption (Fig. 3B). At pH 5 and 7, dBSA adsorption is however importantly reduced, by about 30 and 50% respectively, compared to BSA adsorption. dBSA adsorption at these pH values is moreover almost independent of I. The decreased adsorption of dBSA compared to BSA on AH2 shows that phosphate groups play a role in the adsorption mechanism on that adjuvant, and thus suggests that ligand exchanges are involved. The different behavior of AH1 and AH2 towards the adsorption of dBSA must be explained by different physicochemical properties of these adjuvants, even though our previous works (Art et al., 2017; Art, 2018) did not reveal much difference between them (see Experimental section).

Dephosphorylated ovalbumin (dOVA) was also adsorbed on immobilized AH particles. Mean values (isoresponse maps and $\Delta f_{dOVA\text{-}AH}/\Delta f_{AH}$ ratios) and the corresponding standard deviations for the adsorption of dOVA on both AH adjuvants are shown in SI-6 (Fig. S-6, Tables S-7 and S-8). Fig. 4 presents isoresponse maps of the ratio between the adsorption of dOVA molecules (expressed as $\Delta f_{dOVA\text{-}AH}/\Delta f_{AH}$) on each AH adjuvant and the adsorption of OVA molecules (expressed as $\Delta f_{OVA\text{-}AH}/\Delta f_{AH}$, and presented in Fig. 2) on the same adjuvants. These maps show that the adsorption of dOVA is not statistically different from OVA adsorption on AH1 whatever the conditions of pH and I. On AH2, no statistical difference is observed at pH 5 and 7, and adsorption of dOVA at pH 3 slightly increases compared to OVA adsorption in the same conditions.

dOVA was shown to have 24% less phospho-amino acid residues than native OVA, but its adsorption is similar to OVA on both AH samples. This result suggests no or a minor involvement of ligand exchange in adsorption, or more probably a too low dephosphorylation of

OVA molecules to affect their adsorption. This latter explanation holds even more if an important population of OVA molecules bearing two phosphate groups is present, in which case the removal of the phosphate group from Ser 68, which is accessible to the enzyme, still leaves the molecule with a phosphate group on Ser 344, located inside the protein structure. The latter could be involved in ligand-exchange occurring after protein relaxation at the interface. It was indeed shown that OVA became resistant to elution from AH particles as the vaccine aged (Shi et al., 2001). The use of an alkaline phosphatase could be envisioned in the future to increase the level of dephosphorylation (Kinoshita-Kikuta et al., 2012).

3.4. Desorption of native proteins by phospho-amino acids

Native BSA, HSA or OVA were adsorbed on AH particles immobilized on QCM sensors. Then, the adsorbed layer was submitted to a flow of 55 µg/mL followed by 550 µg/mL of mixed solutions of phospho-amino acids (PO_4-Ser and PO_4-Thr). Depending on the conditions of pH and I, PO_4-AA promoted BSA desorption more or less strongly (Fig. 5A and B). The desorption was the highest (reaching 30% and more) at pH 3 in ultrapure water, *i.e.* in conditions of electrostatic repulsion between BSA and AH particles. In these conditions, the adsorption of BSA is the lowest in terms of adsorbed amount and interaction forces are expected to be the weakest. BSA desorption is also important at pH 5 in ultrapure water and at pH 7 in presence of NaCl, *i.e.* for conditions in which the mechanisms of BSA adsorption on AH particles cannot be explained only by electrostatic interactions (Art et al., 2018). Control experiments conducted with solutions of non-phosphorylated amino acids (AA) show that almost no desorption of previously adsorbed BSA is observed under the action of free serine and threonine (Fig. 5C and D). BSA desorption from AH particles by free PO_4-AA is thus clearly attributed to the presence of PO_4 groups on the free amino acids used for desorption.

The same experiments were conducted with HSA and OVA. The behavior of HSA regarding desorption by PO_4-AA or AA solutions was very similar to the one of BSA (see SI-7 and Fig. S-7). OVA desorption maps are presented in Fig. 6. Almost no desorption of OVA is observed at pH 3. At pH 5 and 7, OVA desorption is only important at low I (in ultrapure water or at 60 mM in NaCl), for both AH adjuvants, *i.e.* for conditions in which OVA adsorption was low. Again, no desorption is observed with non-phosphorylated AA (result not shown) and desorption is thus attributed to the presence of PO_4 groups on free amino acids.

By comparing the desorption maps of BSA and OVA by free PO_4-AA and AA solutions, three conclusions can be drawn. First, protein desorption is related to the presence of phosphate groups on the free amino acids, as non-phosphorylated amino acids do not promote BSA, HSA or OVA desorption. The desorption may tentatively be attributed to the adsorption of free phospho-amino acid molecules through PO_4-OH ligand exchange on AH particles, thereby displacing previously adsorbed proteins. Second, BSA and OVA may have a different principal adsorption mechanism, as the desorption by free PO_4-AA is different for these proteins for a given condition of pH and I. Third, the interaction between phosphate groups of PO_4-AA and AH adjuvant particles differs between AH1 and AH2 adjuvants, as indicated by the lower BSA, HSA and OVA desorption from AH2 particles compared to AH1 particles.

Desorption of BSA, HSA and OVA by PO_4-AA finally suggests that ligand exchanges could be involved in protein adsorption, thanks to the phosphorylated residues of these proteins. However, it is not possible to safely conclude that free PO_4-AA solely replace proteins adsorbed through ligand exchanges, as they could as well compete with other protein-AH surface interactions.

The comparison of results from both types of experiment, *i.e.* adsorption of dephosphorylated proteins and desorption of native proteins with free PO_4-AA is not bringing additional information. Indeed, the conditions in which the desorption of BSA was promoted by free PO_4-AA cannot be related to the conditions in which dBSA adsorption was decreased compared to the one of native BSA. It should however be noted that the system is not challenged the same way in these two cases, as desorption occurs after the protein has relaxed on the surface, while adsorption of dBSA rather highlights the first events of protein adsorption. In the case of OVA, adsorption of dOVA was similar to the one of native OVA, making comparison with OVA desorption by free PO_4-AA non relevant.

3.5. Adsorption of native BSA on KH_2PO_4-treated AH particles

AH-covered sensors were rinsed in the QCM device with a KH_2PO_4 solution prior to BSA adsorption. The objective was to exchange PO_4 groups with OH groups of AH particles, in order to decrease the subsequent adsorption of BSA through ligand exchanges, as proposed by Iyer et al. (2003) and further used by Hansen et al. (2009). AH-covered sensors treated this way were analyzed by XPS to determine the amount of PO_4 groups present at the surface of adjuvant particles after treatment. Results are presented in Table 2.

The most important effects of the treatment of AH with KH_2PO_4 are the appearance of a phosphorus signal and the occurrence of a higher fraction of oxygen bound to aluminum or phosphorus (O—(Al,P)). Note that the binding energy of O—P bonds cannot be distinguished from the one of O—Al bonds. These effects confirm the substitution of hydroxyl groups of AH with PO_4 groups. The observed differences of gold and carbon content can be explained by the variability of sensor coverage by AH particles and of organic contamination, respectively. The Al/O—(Al,P) ratio of untreated samples shows values around 0.33, as expected for aluminum hydroxide. This ratio becomes however somewhat lower after treatment with KH_2PO_4, which is attributed to the substitution of

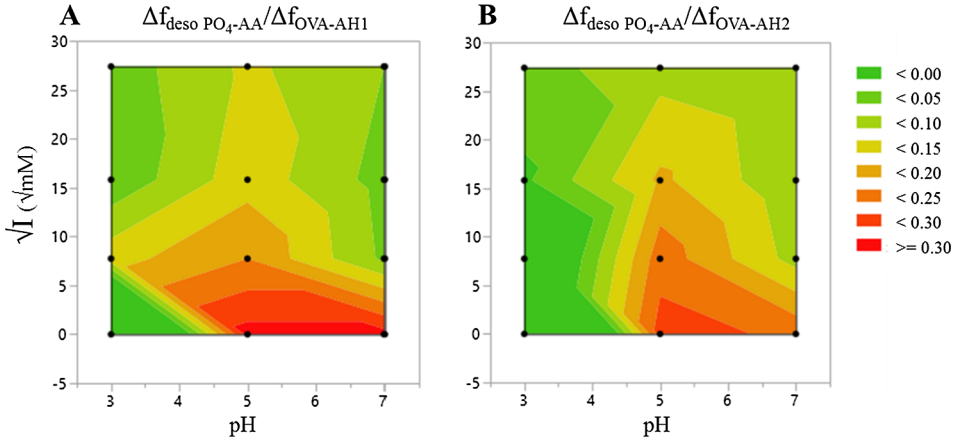

Fig. 6. OVA desorption measured as the ratio of OVA desorbed after treatment with the 550 µg/mL PO_4-AA solution ($\Delta f_{deso\ PO4\text{-}AA}$) and OVA adsorption frequency shift (Δf_{OVA}) on (A) AH1 and (B) AH2 particles. Ratios are presented as a function of pH and square root of ionic strength. Black dots present experimental data (n = 1). Color lines are drawn between experimental data using a triangulation method and linear interpolation. (For interpretation of the references to colour in this figure legend, the reader is referred to the web version of this article.)

Table 2
Surface elemental composition, determined by XPS, of AH particles immobilized on QCM sensors, treated by NaCl and analyzed as such or further rinsed with KH_2PO_4 0.2 M. Results are means for n ≥ 3 (RSD Al ~ 1–4%, RSD O ~ 1.5–4%). "bdl" stands for "below detection limit", as observed on the survey spectra. The oxygen fraction was divided in contributions from O—(Al,P) and O—C bonds as described previously (Art et al., 2017; Art, 2018).

		Al	O—(Al,P)	O—C	C	Au	P	Al/O—(Al,P)	P/Al
AH1	No KH_2PO_4	16.67	50.81	4.30	24.19	4.04	bdl	0.328	–
	After KH_2PO_4	16.98	56.71	3.52	19.86	2.29	0.64	0.299	0.038
AH2	No KH_2PO_4	20.86	58.56	3.75	15.79	0.25	bdl	0.356	–
	After KH_2PO_4	18.66	61.94	2.95	15.71	0.18	0.55	0.301	0.029

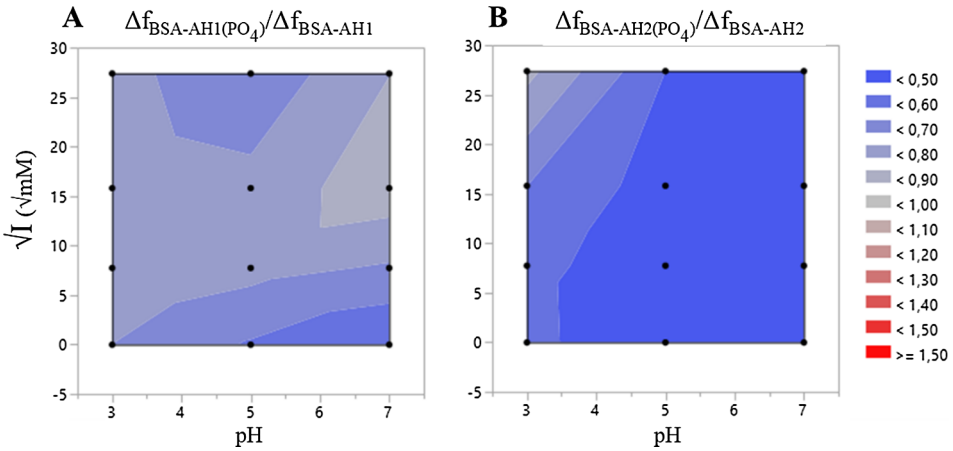

Fig. 7. Ratio of BSA adsorption frequency shifts on KH_2PO_4-treated vs untreated QCM sensors coated with (A) AH1 or (B) AH2 adjuvant particles. Data are presented as a function of pH and square root of ionic strength. Black dots are means of experimental data (n = 1 for BSA-AH (PO_4), n = 5 for BSA-AH), between which color lines are drawn using a triangulation method and linear interpolation. (For interpretation of the references to colour in this figure legend, the reader is referred to the web version of this article.)

hydroxyl groups by phosphate groups and the subsequent higher oxygen amount.

BSA was then adsorbed on KH_2PO_4-treated AH particles. The results obtained for both AH adjuvants are presented in SI-8 (Fig. S-8, Tables S-9 and S-10). The ratio between the frequency shifts of BSA adsorbed on KH_2PO_4-treated AH particles and on untreated AH-covered sensors is presented for all pH and I conditions as an isoresponse map for each AH adjuvant in Fig. 7.

BSA adsorption on KH_2PO_4-treated AH1 particles is decreased in all conditions of pH and I compared to BSA adsorption on untreated AH1 particles. This decrease is however less marked at pH 7 and high I. With AH2, BSA adsorption is strongly reduced at pH 5 and 7 whatever the I value, but remains high at pH 3 and 750 mM in NaCl. The map obtained for BSA adsorption on KH_2PO_4-treated AH2 particles is actually very similar to the one presenting the adsorption of dBSA on AH2 particles. It means that treating AH2 particles with KH_2PO_4 has the same effect on BSA adsorption than reducing the PO_4 content in BSA by 80%. According to the literature, the exposure of AH particles to phosphate groups is believed to have two effects: first it will decrease the number of OH groups available to perform ligand exchange (Iyer et al., 2003), and second it will decrease the PZC of AH particles (Iyer et al., 2003). Treatment with phosphate groups was on the other hand shown to have no effect on the surface area, the morphology or the AH particle size (Chang et al., 1997).

The work of Iyer et al. is particularly interesting to further discuss the effect of the substitution of OH groups of AH adjuvants by phosphate groups and the associated decrease of PZC (Iyer et al., 2003). In that work, AH adjuvants were produced with various degrees of phosphate substitution. For each produced adjuvant, the amount of adsorbed phosphate groups was evaluated by difference between the initial added amount and remaining amount in the supernatant after centrifugation using ICP-AES. The PZC of each adjuvant was measured using electrophoretic mobility measurements at various pH values. According to their results, the PZC of AH adjuvants, initially around 11.5, decreases to ~10.5 and ~9 for PO_4-substituted amounts of 0.0326 and 0.1211 mg PO_4/mg Al, *i.e.* 0.009 mol PO_4/mol Al and 0.034 mol PO_4/mol Al, respectively.

In the present work, XPS data reveal that the KH_2PO_4 treatment of AH-covered sensors leads to the presence of 0.038 and 0.029 mol PO_4/mol Al at the surface of AH1 and AH2 particles, respectively (see P/Al ratio in Table 2). AH1 and AH2 have an initial PZC that was measured around 9.7 and 10, respectively (Art, 2018). After KH_2PO_4 treatment, the PO_4/Al ratio is in the range of the value of 0.034 mol PO_4/mol Al obtained by Iyer et al. which led to a very significant drop of the PZC. The PZC of AH1 and AH2 adjuvants is thus expected to be significantly reduced and to get closer to the higher pH values used here for adsorption. This decrease would thus mainly impair electrostatic interactions at pH 7 if they were involved, which seems however not to be the case (see Fig. 1). At lower pH values (3 and 5), electrostatic interactions should not be much affected. Since adsorption was also decreased on KH_2PO_4-treated AH2 at pH 5, and since electrostatic interactions cannot explain adsorption at pH 7, the observed decrease of BSA adsorption on AH particles after KH_2PO_4 treatment may thus be explained by the PO_4-OH substitution, which decreases the number of sites available to perform ligand exchanges on AH particles, and may thus impair protein adsorption through this latter mechanism.

It should be noted that when dephosphorylated proteins were used, their adsorption was performed in presence of the free phosphate groups released by the action of PAP. The free phosphate concentration in the dephosphorylated protein solutions is however of the order of 10^{-7} M and 10^{-6} M for dBSA and dOVA, respectively (computed based on Table 1). These concentrations are many orders of magnitude lower than the value of 0.2 M used for KH_2PO_4 treatment, and cannot induce a marked decrease of PZC, as also verified by comparing the amount of free phosphates available throughout a QCM experiment to the mass of aluminum deposited on each sensor (not shown).

3.6. General discussion

The involvement of ligand exchanges in protein adsorption on AH adjuvants was challenged using three approaches: (i) comparison of the adsorption of native and dephosphorylated proteins, (ii) tentative desorption of adsorbed proteins using free PO_4-AA, and (iii) adsorption of proteins on AH particles that were previously treated with phosphate

ions. In each case, there are conditions of pH and I in which significant alterations of adsorption are observed, with variations according to the adjuvant used (AH1 vs AH2) and according to the nature of the protein (BSA/HSA vs OVA). Taken together, the results thus highlight the importance of ligand exchanges in the adsorption mechanism of proteins on AH adjuvants. As it was shown that the strong binding of antigens to AH adjuvants occurring through ligand exchange leads to a decreased immune response (Hansen et al., 2009), the reported data have a high significance for the development of efficient vaccines.

The comparison of these three approaches is however not straightforward since approaches (i) and (iii) are related to the initial affinity of the protein for the interface with, in (i), changes brought to the protein, and in (iii), changes brought to the interface, while approach (ii) challenges the protein-surface interactions occurring once relaxation of the protein at the interface may have occurred. Actually, there is an agreement between the results of approaches (i) and (iii), revealing a stronger influence of ligand exchanges for BSA at pH 7, low I and on AH2. The fact that desorption by PO_4-AA (approach (ii)) is more pronounced on AH1 at pH 3, low I or pH 7, high I, *i.e.* in conditions opposite to the ones in which BSA-AH affinity would be driven by ligand exchanges, may be the result of the fact that desorption by PO_4-AA rather challenges other interactions that are actually weaker. When the protein is adsorbed mostly through ligand exchanges, PO_4-AA are not able to displace it, while when it is adsorbed through other mechanisms, the strong free PO_4-AA – AH interaction replaces weaker protein-AH interactions.

The results reveal important differences between BSA (or HSA) and OVA adsorption. In the literature, these differences are explained by a driving force for adsorption respectively based on electrostatic interactions and ligand exchanges for BSA and OVA (Hem et al., 1995; Al-Shakhshir et al., 1995; Kinoshita-Kikuta et al., 2012; Morefield et al., 2005). Our results bring more nuances to the adsorption mechanism as it appears that electrostatic interactions cannot fully explain the behavior of BSA (see in particular the effect of ionic strength at pH 7) (Art et al., 2018), and that despite a very low level of phosphorylation of BSA molecules, ligand exchanges do play a role in BSA adsorption, at least in some conditions. The concentration of BSA molecules bearing a phosphate group is very low (less than 6% in average). At the onset of adsorption, the surface must then be populated in majority by non-phosphorylated BSA molecules. With time however, if the affinity of phosphorylated BSA molecules for the surface is higher, the latter may displace non-phosphorylated molecules according to the Vroman effect (Bingham et al., 1976), resulting in a stronger BSA-surface interaction that cannot be challenged by free PO_4-AA.

The results also highlight differences between AH1 and AH2, even though a detailed physicochemical characterization of these two adjuvants did not reveal striking differences between them (see Experimental section). Proteins thus here serve as probes to reveal subtle differences between adjuvants that are not otherwise easily approached. Progress in the characterization of AH adjuvants are still to be made, notably regarding their ability to exchange ligands.

4. Conclusion

The QCM platform developed in a previous work (Art et al., 2018) and based on the immobilization of aluminum hydroxide adjuvant particles on QCM sensors has been used to further explore the adsorption mechanisms of model proteins on commercial vaccine adjuvants, with the focus set on ligand exchanges. The adsorption of native and dephosphorylated protein molecules allowed to demonstrate the involvement of PO_4-OH ligand exchanges in BSA adsorption on AH particles, while this was already previously proposed in the literature for OVA adsorption only. This mechanism may thus be involved even in case of low phosphate content in the protein. Treating AH adjuvants with PO_4 groups prior to BSA adsorption also reduced the latter in the same conditions that were affected by BSA dephosphorylation. Free phosphorylated amino acids were shown to desorb BSA and OVA. This was in particular the case for BSA in pH and I conditions in which ligand exchanges were not revealed by the other experiments, suggesting that free PO_4-AA rather displace BSA molecules adsorbed through weaker interactions.

This work globally shows that BSA and OVA molecules adsorb to AH adjuvants through several mechanisms, among which ligand exchanges, more or less involved depending on pH and I conditions. This brings nuances to previous works, which concluded that BSA and OVA adsorption on AH adjuvant was mainly driven respectively by electrostatic interactions and by ligand exchanges. The results also highlight the fact that the two tested commercial adjuvants behave quite differently towards protein adsorption despite their similar physicochemical properties. Progresses are still to be made in the characterization of AH adjuvants, with a view to elucidate the link between their characteristics and antigen adsorption. The direct study of antigen adsorption on AH used in formulation, notably using the QCM platform we developed, may actually constitute an efficient way to reveal subtle differences between adjuvants.

This new method of studying vaccine components and antigen adsorption has finally proven its efficacy to directly record adsorbed antigen amounts, as well as its usefulness to study the desorption of adsorbed proteins from AH adjuvant particles. The QCM experiments conducted in the present work could be expanded to understand more precisely the effects of the *in vivo* conditions found after injection on vaccines formulated with antigens adsorbed on adjuvant particles. The desorption of antigens from adjuvant particles could indeed be studied in a very large range of conditions, thanks to this platform.

Declaration of Competing Interest

The authors declare that they have no known competing financial interests or personal relationships that could have appeared to influence the work reported in this paper.

Acknowledgments

The authors thank the BRENNTAG company for kindly providing the ALHYDROGEL® '85' material. Many thanks to the Environmental Sciences division (ELIE) of the Earth and Life Institute (ELI), and particularly to Anne Iserentant, for the ICP-AES analyses. The authors also acknowledge the jury members of the PhD thesis of Jean-François Art (Caroline Dekeyser, Jacques Devaux, Grégory Francius, Eric Gaigneaux and Véronique Préat) for their critical opinion on the manuscript.

Appendix A. Supplementary material

Supplementary data to this article can be found online at https://doi.org/10.1016/j.ijpharm.2019.118834.

References

Al-Shakhshir, R.H., Regnier, F.E., White, J.L., Hem, S.L., 1995. Contribution of electrostatic and hydrophobic interactions to the adsorption of proteins by aluminium-containing adjuvants. Vaccine 13, 41–44.
Art, J.-F., 2018. Quartz crystal microbalance sensors to elucidate interaction mechanisms between antigens and aluminum-based vaccine adjuvants. IMCN, Université catholique de Louvain, UCL, pp. 282.
Art, J.-F., vander Straeten, A., Dupont-Gillain, C.C., 2017. NaCl strongly modifies the physicochemical properties of aluminum hydroxide vaccine adjuvants. Int. J. Pharmaceut. 517, 226–233.
Art, J.-F., vander Straeten, A., Dupont-Gillain, C.C., 2018. Immobilization of aluminum hydroxide particles on quartz crystal microbalance sensors to elucidate antigen–adjuvant interaction mechanisms in vaccines. Anal. Chem. 90, 1168–1176.
Bingham, E.W., Farrell, H.M., Dahl, K.J., 1976. Removal of phosphate groups from casein with potato acid phosphatase. Biochim. Biophys. Acta (BBA) - Enzymology 429, 448–460.
Burrell, L.S., Lindblad, E.B., White, J.L., Hem, S.L., 1999. Stability of aluminium-containing adjuvants to autoclaving. Vaccine 17, 2599–2603.
Burrell, L.S., White, J.L., Hem, S.L., 2000. Stability of aluminium-containing adjuvants

during aging at room temperature. Vaccine 18, 2188–2192.
Chang, M.F., White, J.L., Nail, S.L., Hem, S.L., 1997. Role of the electrostatic attractive force in the adsorption of proteins by aluminum hydroxide adjuvant. PDA J. Pharm. Sci. Technol. 51, 25–29.
Clausi, A., Cummiskey, J., Merkley, S., Carpenter, J.F., Braun, L.J., Randolph, T.W., 2008. Influence of particle size and antigen binding on effectiveness of aluminum salt adjuvants in a model lysozyme vaccine. J. Pharm. Sci. 97, 5252–5262.
Eppstein, D.A., Byars, N.E., Allison, A.C., 1989. Use of peptides and proteins as drugs, Part I New adjuvants for vaccines containing purified protein antigens. Adv. Drug Deliv. Rev. 4, 233–253.
Hansen, B., Belfast, M., Soung, G., Song, L., Egan, P.M., Capen, R., HogenEsch, H., Mancinelli, R., Hem, S.L., 2009. Effect of the strength of adsorption of hepatitis B surface antigen to aluminum hydroxide adjuvant on the immune response. Vaccine 27, 888–892.
Hem, S.L., White, J.L., 1995. Stucture and properties of aluminum-containing adjuvants. In: Powell, M.F., Newman, M.J. (Eds.), Vaccine Design : The Subunit and Adjuvant Approach. Plenum Press, New York, pp. 249–276.
Iyer, S., HogenEsch, H., Hem, S.L., 2003. Effect of the degree of phosphate substitution in aluminum hydroxide adjuvant on the adsorption of phosphorylated proteins. Pharm. Dev. Technol. 8, 81–86.
Jachimska, B., Pajor, A., 2012. Physico-chemical characterization of bovine serum albumin in solution and as deposited on surfaces. Bioelectrochemistry 87, 138–146.
Jachimska, B., Tokarczyk, K., Łapczyńska, M., Puciul-Malinowska, A., Zapotoczny, S., 2016. Structure of bovine serum albumin adsorbed on silica investigated by quartz crystal microbalance. Colloids Surf., A 489, 163–172.
Jiang, D., Morefield, G.L., HogenEsch, H., Hem, S.L., 2006. Relationship of adsorption mechanism of antigens by aluminum-containing adjuvants to in vitro elution in interstitial fluid. Vaccine 24, 1665–1669.
Johnston, C.T., Wang, S.-L., Hem, S.L., 2002. Measuring the surface area of aluminum hydroxide adjuvant. J. Pharm. Sci. 91, 1702–1706.
Kinoshita-Kikuta, E., Kinoshita, E., Koike, T., 2012. Separation and identification of four distinct serine-phosphorylation states of ovalbumin by Phos-tag affinity electrophoresis. Electrophoresis 33, 849–855.
Mbow, M.L., De Gregorio, E., Valiante, N.M., Rappuoli, R., 2010. New adjuvants for human vaccines. Curr. Opin. Immunol. 22, 411–416.
Mc Evoy, K., 2012. Improving quantification of proteins at interfaces through a better and practical modeling of Quartz Crystal Microbalance response. Université catholique de Louvain.
Morefield, G.L., HogenEsch, H., Robinson, J.P., Hem, S.L., 2004. Distribution of adsorbed antigen in mono-valent and combination vaccines. Vaccine 22, 1973–1984.
Morefield, G.L., Jiang, D., Romero-Mendez, I.Z., Geahlen, R.L., HogenEsch, H., Hem, S.L., 2005. Effect of phosphorylation of ovalbumin on adsorption by aluminum-containing adjuvants and elution upon exposure to interstitial fluid. Vaccine 23, 1502–1506.
Nakamura, K., Era, S., Ozaki, Y., Sogami, M., Hayashi, T., Murakami, M., 1997. Conformational changes in seventeen cystine disulfide bridges of bovine serum albumin proved by Raman spectroscopy. FEBS Lett. 417, 375–378.
Nattich-Rak, M., Sadowska, M., Adamczyk, Z., Cieśla, M., Kąkol, M., 2017. Formation mechanism of human serum albumin monolayers on positively charged polymer microparticles. Colloids Surf., B 159, 929–936.
Norde, W., 2008. My voyage of discovery to proteins in flatlandand beyond. Colloids Surf., B 61, 1–9.
Perrie, Y., Mohammed, A.R., Kirby, D.J., McNeil, S.E., Bramwell, V.W., 2008. Vaccine adjuvant systems: Enhancing the efficacy of sub-unit protein antigens. Int. J. Pharm. 364, 272–280.
Rinella Jr, J.V., White, J.L., Hem, S.L., 1998. Effect of pH on the elution of model antigens from aluminum-containing adjuvants. J. Colloid Interface Sci. 205, 161–165.
Salis, A., Boström, M., Medda, L., Cugia, F., Barse, B., Parsons, D.F., Ninham, B.W., Monduzzi, M., 2011. Measurements and theoretical interpretation of points of zero charge/potential of BSA protein. Langmuir 27, 11597–11604.
Shi, Y., HogenEsch, H., Hem, S.L., 2001. Change in the degree of adsorption of proteins by aluminum-containing adjuvants following exposure to interstitial fluid: freshly prepared and aged model vaccines. Vaccine 20, 80–85.
Shirodkar, S., Hutchinson, R.L., Perry, D.L., White, J.L., Hem, S.L., 1990. Aluminum compounds used as adjuvants in vaccines. Pharm. Res. 7, 1282–1288.
Sivakumar, S.M., Safhi, M.M., Kannadasan, M., Sukumaran, N., 2011. Vaccine adjuvants – Current status and prospects on controlled release adjuvancity. Saudi Pharmaceut. J. 19, 197–206.
Wittayanukulluk, A., Jiang, D., Regnier, F.E., Hem, S.L., 2004. Effect of microenvironment pH of aluminum hydroxide adjuvant on the chemical stability of adsorbed antigen. Vaccine 22, 1172–1176.